Numerical simulation of particulate-flow in spiral separators (15 % solids)

Mahran, G. M. A.[*1], Doheim, M. A.[**], AbdelGawad, A.F[*,2], Abu-Ali, M. H.[**], Rizk, A.M.[**]**

[*] King Abdulaziz University, Jeddah 21589,Saudi Arabia.

[**]Mining and Metallurgical Eng. Dept., Faculty of Engineering, Assiut University, Egypt.

[***] Mechanical Power Eng. Dept., Faculty of Engineering, Zagazig University, Egypt.

[2]Currently: Mech. Eng. Dept., Umm Al-Qura University, Makkah, Saudi Arabia

Simulación numérica del flujo de partículas en un separador espiral (15 % de sólidos)

Simulació numèrica del fluix de partícules en un separador d'espiral (15% de sòlids)

Recibido: 6 de febrero 2014; revisado: 7 de octubre de 2014; aceptado: 5 de noviembre de 2014

RESUMEN

El separador espiral es un dispositivo de concentración por gravedad. Fue inventado por Humphreys in 1941.Ha sido diseñado y desarrollado en base a la experiencia y a la gran variedad de prototipos y modificaciones. El objetivo principal del presente estudio es la simulación del flujo de partículas de concentraciones de sólidos más reales (15% de sólidos en peso) en un separador espiral. El estudio se ha basado en el método Eulerian y el modelo de turbulencia RNG K-ε. Los resultados se centran en las características del flujo de partículas como la velocidad y la distribución y concentración de partículas en la curvatura espiral. Los resultados pronosticados se comparan con los valores experimentales en el caso de una espiral de carbón tipo LD9. Las comparaciones entre los datos numéricos y los medidos coinciden bastante.

Palabras clave: Separador de espiral, flujo de partículas, simulación numérica, modelo de turbulencia, separación por gravedad, CFD.

SUMMARY

Spiral separator is a gravity concentration device. It was invented by Humphreys in 1941.It is firstly designed and developed based on experience and through many testing of prototypes and modifications. The main objective of the present study is simulation of the particulate-flow of more realistic solids concentration (15% solids by weight) in spiral separator. The study is based on Eulerian approach and RNG K-ε turbulence modeling. The results focus on particulate-flow characteristics such as velocity, and distribution and concentration of particulates on the spiral trough. The predicted results are compared with the experimental in case LD9 coal spiral. Comparisons between numerical and measured data show good agreement.

Key words: Spiral separator, particulate-flow, numerical simulation, turbulence modeling, gravity separation, CFD.

RESUM

Un separador d'espiral és un dispositiu de concentració per gravetat. Va ser inventat per Humphreys en 1941. Va ser dissenyat i desenvolupat en primer lloc sobre la base de l'experiència i a través de moltes proves de prototips i modificacions. L'objectiu principal d'aquest estudi és la simulació del fluix de partícules de concentració de sòlids més real (15% de sòlids en pes) en un separador d'espiral. L'estudi es basa en el mètode Eulerian i el model de turbulència RNG K-ε. Els resultats corresponen a les característiques del fluix de partícules, com la velocitat i la distribució i concentració de partícules al canal espiral. Els resultats predits es comparen amb els valors experimentals en el cas d'un espiral de carbó LD9. Les comparacions entre les dades numèriques i les mesurades coincideixen bastant.

Paraules clau: Separador d'espiral, fluix de partícules, simulació numèrica, model de turbulència, separació per gravetat, CFD

*Corresponding author:1gamalmahran@hotmail.com

INTRODUCTION

A spiral concentrator consists of an open trough that twists downward helically around a central axis. Majority of current designs of spirals have 5 to 7 turns. It is basically a helical sluice, as shown in Fig. (1) Spiral separator is firstly designed and developed based on experience and through many testing of prototypes and modifications. Because of the simplicity of operation and low cost, spirals have been widely used in the mineral industry to separate high-density particles from low-density ones. Development of any spiral design remains largely a process of trial and error. To reduce development time and costs, many experimental models of the spiral were made. Traditionally a spiral separator has been used effectively in the coal and beach sand industries. Currently, it is successfully used to beneficiate a number of ores such as chromite, rutile, gold ore, iron ore, mainly due to its operational simplicity and cost effectiveness. Recently, there has been an accelerated growth in the use of spirals for iron ore beneficiation. The demand for higher efficiency of separation is compromised by a higher capacity in the size range of 3 mm to 45 μm. For iron ore beneficiation, this size range is considered coarse to be treated by floatation and it is considered fine for other conventional gravity separators like jig which performs better for feed materials above 2 mm size. Despite all its advantages, there has been an increased demand to design spirals to accommodate feed materials that vary oversize as well as grade. So, the challenge has been to design the correct profile of the spiral. Since its inception, a lot of work has been done to understand and improve the performance of spirals (Mishra and Tripathy, 2010; Holland-Batt,1995; Machunter et al., 2003; Gulsoy and Kademli,2006; Jancar et al. 1995), However, to predict the performance of a spiral for any given application, and more importantly, to design spirals for a particular ore type to obtain a desired grade, a lot of experiments must be done. These are quite cumbersome and costly. Hence, there are many options in the simulation of the separation process in spiral separators.

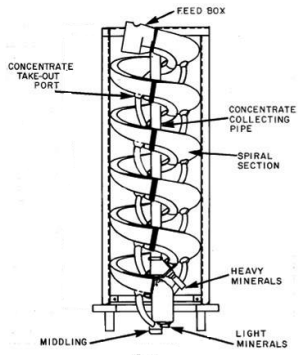

Fig. (1) *A Humphreys spiral.*

Mathematical models are therefore of great value for determining how such flows are influenced by fluid properties and geometrical parameters and, hence, for predicting and improving the performance of these separators (Stokes et al.,2004; Ferziger and Peric, 1999; Loveday and Cilliers,1994; Kuang et al, 2014; Radman et al,2014). These models started by Burch (1962) when he assumed the pulp to be a liquid of uniform viscosity. He also assumed that the secondary flow would not affect the primary flow. Wang and Andrews (1994) introduced a first step in the development of a mechanistic model of the spiral operation. The model determines the flow fields for simplified rectangular spiral sections. Jancar et al (1995) investigated the fluid flow on LD9 spiral using their developed code. All these models were developed with time to be more reliable. Mathews et al. (1998a,1998b,1999a,1999b) presented CFD modeling of the fluid flow on spiral trough. Doheim et al.(2013) suggested CFD model based on Eulerian approach and turbulence model in case of low solid concentration from 0.3 to 3% solids by weight.

The present paper followsthe overall CFD modeling fluid-particle flow in gravity concentrators in spiral separators. The discussions are concentrated on the adoption of realistic solid percent in spiral separatorsof multiphase flow models as well as model validation against experimental data.The present study suggests a particulate-flow computational model based on Eulerian approach. The present model is validated using the experimental data of LD9 spiral (Holland-Batt and Holtham,1991; Holtham,1997**;** Holtham, 1992). The main objective of this study is to obtain a comprehensive mathematical model according to Computational Fluid Dynamics (CFD). The present study will focus on the shortcomings of the previous mathematical models so as to obtain a more accurate and reliable model.

SPIRAL SEPARATOR DESCRIPTION

Spiral Geometry

The design parameters of the spiral separator can be listed as: spiral pitch (υ), profile shape, length (*L*), and inner and outer trough radii (r_i , r_o) that govern the curvature (ψ) of the channel. The parameters are shown in Fig. (2) and defined as follows (Doheim et al.,2013):

Pitch: $u = 2 \pi r \tan(\alpha)$ (m)
Height loss: $h = R r \tan(\alpha)$ (m)
Mainstream distance: $L(r)=R\ r/\cos(\alpha)$ (m)
Curvature: $\psi=(ri+ro)/2W$ (dimensionless)
Trough width: $W=ro–ri$ (m)
Spiral height: $H=n*u$ (m)

Where, *R* is the angular distance in radians in the mainstream direction from the spiral inlet (=2 π , on full turn), *r* is the radial distance from the centerline axis, α is the descent angle, *H* is the spiral height and *W* is the trough width. The geometrical parameters for *LD9* spiral are stated in Table 1 (Doheim et al.,2013).

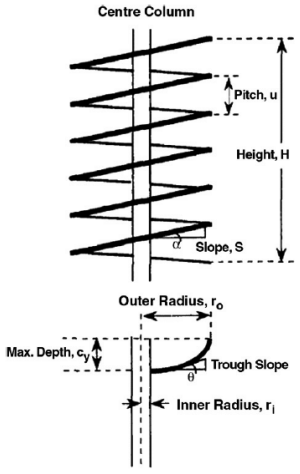

Fig. (2) *Schematic drawing of a spiral separator.*

Table (1) *The geometrical parameters of LD9 spiral separator (Doheim et al.,2013*

Inner Radius r_i(mm)	Outer Radius r_o (mm)	Trough Width *W* (mm)	Pitch u (mm)	Curvature ψ	Descent angle α(°)	Number of Turns *n*
70	350	280	273	0.75	7 - 32	6

Mechanism of Particle Separation

Feed is introduced through the feed box at the top of spiral, which establishes the correct pattern of the flow. The feed enters the spiral trough as a homogenous slurry. The pulp flows spirally downward, the spiral separates minerals in accordance with their specific gravity and particle size. Low density and small size particles remain suspended and travel outwards due to the centrifugal force to accumulate in the outer trough regions, whilst high density and coarse size particles settle in the flow to slide inwards toward the central column (Fig. 3).

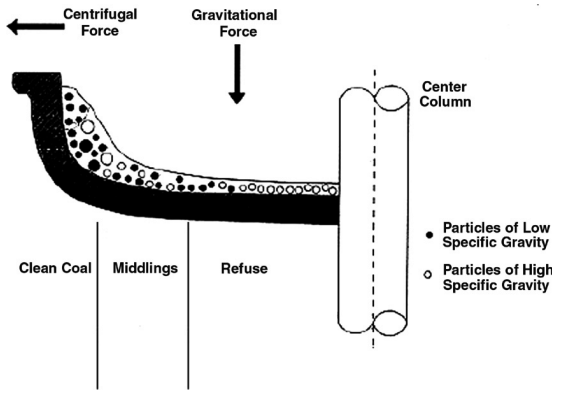

Fig. (3) *Cross section of spiral trough.*

GOVERNING EQUATIONS AND NUMERICAL DESCRIPTION OF THE MODEL

GOVERNING EQUATIONS

To model particulate-flow on a spiral separator, two-phase flow (water and solid) is considered. The continuity and momentum equations are used for multiphase (water and solid) flow throughout the domain. The flow on a spiral separator is considered to be Newtonian and turbulent. Continuity and *Navier–Stokes* equations supplemented by a suitable turbulence model are appropriate for modeling the spiral separator flow. The following transient equations describe the conservation of mass and momentum equations.

Continuity Equation

The continuity equation for phase *q* (ether water or particulate-phase) is

$$\frac{\partial}{\partial t}(\alpha_q \rho_q) + \nabla.(\alpha_q \rho_q \vec{v}_q) = 0 \qquad (1)$$

Where α_q is the volume fraction of phase , q, $\vec{v}_q$ is velocity vector of phase , q, ρ_q is the material density of phase and q is the phase (either water or solid).

Momentum Equations

The momentum equations for two phases ("fluid and particulate" or "water and solids") represent a multi-fluid granular model to describe the flow behavior of a fluid-solid mixture. The solid-phase stresses are derived by making an analogy of the random particle motions arising from particle-particle collisions. The momentum conservation equations for the fluid (liquid (water, ***l***)) and particulate (solids, ***s***) are:

$$\frac{\partial}{\partial t}(\alpha_l \rho_l \vec{v}_l) + \nabla \cdot (\alpha_l \rho_l \vec{v}_l \vec{v}_l) = -\alpha_l \nabla p + \nabla \cdot \overline{\overline{\tau}}_l + \alpha_l \rho_l \vec{g} + \vec{F}_{lift,l} + \sum_{l=1}^{N} R_{sl} \qquad (2)$$

$$\frac{\partial}{\partial t}(\alpha_s \rho_s \vec{v}_s) + \nabla \cdot (\alpha_s \rho_s \vec{v}_s \vec{v}_s) = -\alpha_s \nabla p - \nabla p_s + \nabla \cdot \overline{\overline{\tau}}_s + \alpha_s \rho_s \vec{g} + \vec{F}_{lift,s} + \sum_{l=1}^{N} R_{ls} \qquad (3)$$

Where: $\bar{\bar{\tau}}_q$ is the q^{th} phase stress-strain tensor.

$$\bar{\bar{\tau}}_q = \alpha_q \mu_q \left(\nabla \vec{v}_q + \nabla \vec{v}_q^T\right) + \alpha_q \left(\lambda_q - \frac{2}{3}\mu_q\right) \nabla . \vec{v}_q \bar{\bar{I}} \qquad (4)$$

Where, μ_q and λ_q are the shear and bulk viscosity of phase q, $F_{Lift,q}$ is a lift force, p is the pressure shared by all phases, v_q is velocity of phase velocity of phase q (liquid or solid-particulate phase), v_l is velocity of liquid phase, v_s is velocity of solid phase, and R_{sl} or R_{ls} is an interaction force between phases.

Equations (2 & 3) must be closed with appropriate expressions for the inter-phase force .This force depends on the friction, pressure, cohesion and other effects, and is subject to the conditions that $R_{sl} = -R_{ls}$ and $R_{ll} = 0$.

The simple interaction term is:

$$\vec{R}_{sl} = k_{sl}(\vec{v}_s - \vec{v}_l)$$
$$\vec{R}_{ls} = k_{ls}(\vec{v}_l - \vec{v}_s) \qquad (5)$$

Where, is an interaction force between phases, (=) is the momentum-exchange coefficient between fluid [not "or solid"] phase (l) and solid phase (s), and N is the total number of phases.

$$F_{lift} = -0.5 \rho_q \alpha_p |\vec{v}_q - \vec{v}_p| \times (\nabla \times \vec{v}_q) \qquad (6)$$

TURBULENCE MODELS

Doheimet al. (2013) deduced that RNG-K-ϵ turbulence model is the most accurate turbulence in case of particulate flow of spiral separator modeling. The RNG-K-ϵ turbulence model is derived from the instantaneous Navier-Stokes equations. The derivation is based on a mathematical technique called "renormalization group" (RNG) method (Yakhot and Orszag,1986; Escue and Cui,2010). Transport equations for the RNG K-ϵ model have a similar form to the standard k-ϵ model.

$$\frac{\partial}{\partial t}(\rho k) + \frac{\partial}{\partial x_i}(\rho k u_i) = \frac{\partial}{\partial x_j}\left(\alpha_k \mu_{eff} \frac{\partial k}{\partial x_j}\right) + G_k - \rho \varepsilon \qquad (7)$$

$$\frac{\partial}{\partial t}(\rho \varepsilon) + \frac{\partial}{\partial x_i}(\rho \varepsilon u_i) = \frac{\partial}{\partial x_j}\left(\alpha_\varepsilon \mu_{eff} \frac{\partial \varepsilon}{\partial x_j}\right) + C_{1\varepsilon}\frac{\varepsilon}{k}(G_k) - C_{2\varepsilon}\rho\frac{\varepsilon^2}{k} - R_\varepsilon \qquad (8)$$

The *RNG* turbulence model is more sensitive to the mean rate of strain because of R_e in Eq.8. Where, G_k is the generation of turbulence kinetic energy due to the mean velocity gradient. G_k may be defined as follows:

$$G_k = -\rho \overline{u_i' u_j'} \frac{\partial u_j}{\partial x_i} \qquad (9)$$

Where: $(-\rho \overline{u_i' u_j'})$ terms are known as the Reynolds stresses.

The effective viscosity, μ_{eff}, is given by

$$\mu_{eff} = \mu\left(1 + \sqrt{\frac{C_\mu \rho k}{\mu \sqrt{\varepsilon}}}\right)^2 \qquad (10)$$

Where: μ is dynamic viscosity (kg/ms).

The main difference between the *RNG* and standard *k-ϵ* models lies in the additional term in the ϵ equation and is given by

$$R_\varepsilon = \left\{ \frac{C_\mu \rho \eta^3 (1-\frac{\eta}{\eta_0}) \varepsilon^2}{1+\beta \eta^3} \right\} \frac{\varepsilon^2}{k} \qquad (11)$$

Where, $\eta = S * k/\varepsilon$ and S is the modulus of the mean rate of strain tensor, η_0 and β are constants equal to 4.38 and 0.012, respectively. The model constants are set as $C_{1\epsilon}$ =1.42, $C_{2\epsilon}$=1.68, and C_μ= 0.0845.

COMPUTATIONAL DOMAIN

The computational domain (Fig. 4) is different from that used in low solid percentage (Doheim et al.,2013) This is because the free-surface profile of current domain was taken from experimental investigation (Holtham**,**1992). The free-surface profile formed the upper boundary of the computational domain and thus remained fixed during the coupled water-particle calculation. The computational domain consists of one complete turn of the *LD9* spiral separator. The number of cells are 150 × 40 × 10 in the mainstream, cross-stream and depth-wise directions, respectively. The total number of cells is 60000. The computational grid is a structured mesh consisting of hexahedral control volumes. Careful consideration was paid to minimize the dependence of solution on the mesh by improving the clustering of cells near solid walls until results are almost constant. The investigation was carried out using a different number of cells, namely: 40000, 50000, 60000, 70000 and 80000. It was found that the number of cells in the range of 60000 gives the same results as the higher numbers of cells. The least y+ from the wall for the first node was about 4.

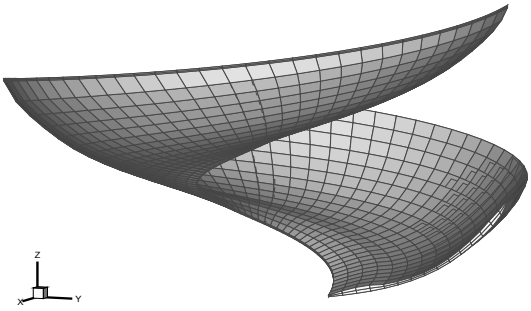

Fig. (4) *Computational domain of LD9 spiral at 6 m³/hr flow rate and 15 % solids in feed with reduced cells for clarity.*

BOUNDARY CONDITIONS

Four boundaries are surrounding the suggested domain, namely: inlet plane, outlet plane, solid walls. At the inlet boundary of the spiral, velocity components and volume fractions of solids are specified to give the desired flow rates of slurry. At the exit of the domain (outlet plane), velocity gradients are set to zero. At the trough bottom, no-slip conditions are suggested for water only. At the top surface of the computational domain, fixed surface is used. The wall-roughness constant is set to 0.5. The water phase on spiral separator is assumed to have constant physical properties. Thus, the assumed properties are ρ_{water} = 1000 *kg/m³*, μ_{water} = 0.0009 *kg/m s*. Table (2) shows the details of densities (and sizes () of used particles.

Table 2: *The properties of used particles*

Particle type	Density (ρ_p) (kg/m³)	Diameter (D_p) (Micrometer)		
Glass beads	2440	75	530	-
Quartz	2650	75	530	1400
Coal	1450	75	530	-

NUMERICAL TREATMENT

The model of particulate-flow uses a time-dependent formulation. The numerical solution is based on finite volume method. The equations were discretized using the Quadratic Upwind Interpolation (QUICK) scheme. The equations were solved with the unsteady solver with a time step of 0.001 sec. Residuals of all variables were restricted to 1×10-5. A validated commercial code (Fluent 6.3.26 User's Guide, 2006) was used to solve the above equations of the model.

RESULTS AND DISCUSSIONS

In the present work, the numerical predictions of particulate-flow in LD9 spiral separator at flow rate of 6 m3/hr are compared with the experimental results (Holland-Battand Holtham,1991; Holtham,1997; Holtham, 1992). The available experimental data to validate the numerical results are given in a certain part (stream) on the spiral trough. The number of streams on spiral trough are eight streams. It means that the spiral trough is divided into eight streams by putting seven splitters as shown in Figure (5). The model is investigated at realistic solid percentage (15%) using RNG k-ε model (most accurate turbulence model, (Doheim et al.,2013). The particulate-flow parameters are shown in the following sections. The used particles in this case are shown in Table (3).

Table 3: *The used particles in the case of 15 % solids.*

Particles Type	Density (ρ)	Size (μm)	Mix ratio
Coal	1450	75	2
Coal	1450	530	2
Quartz	2650	75	1
Quartz	2650	530	1

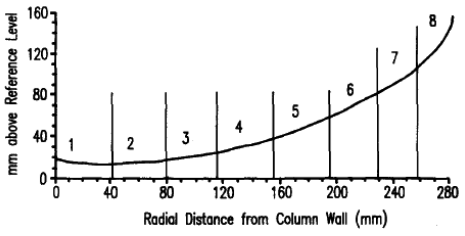

Fig.(5) *Eight sampling streams employed on the spirals.*

Particle concentrations

Figure (6) shows the predicted and experimental (Holland-Batt and Holtham, 1991;Holtham,1992) values of

particle concentrations by volume in each stream. There is a good agreement between the predicted and the experimental values as shown in Figure.

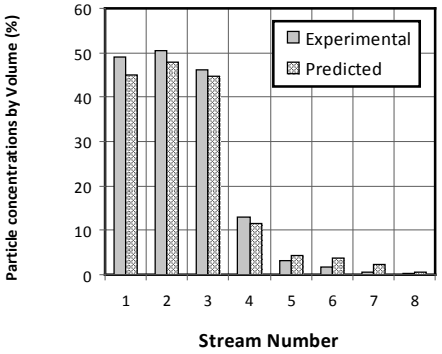

Fig. (6) *Predicted and experimental (Holland-Batt and Holtham, 1991; Holtham,1992) values of particle concentrations by volume in each stream, 15% solids in feed.*

PULP VELOCITY

The predicted mean-stream pulp velocity for 15% solids is shown in Fig. (7).The mean-stream pulp velocity increases smoothly in the outward-direction away from the centerline of the spiral trough. The predicted pulp-velocity contours are shown in Fig.(8).

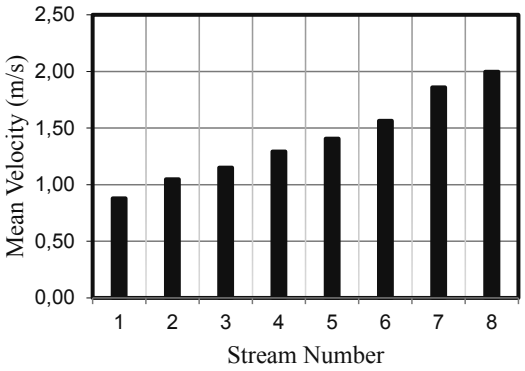

Fig.(7) The predicted values of mean-stream pulp velocity, at 15 % solids.

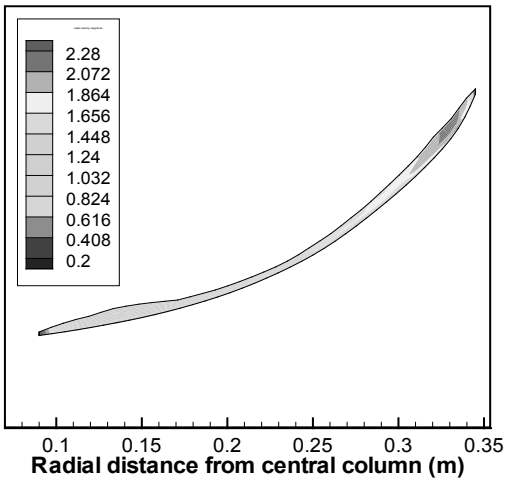

Fig.(8) *The predicted pulp-velocity contours (m/s), at 15 % solids.*

STREAM FLOW- RATE

The predicted values of stream flow-rate are shown in Fig. (9). It is clear from the figure that the stream flow-rate values depend on the cross-sectional area and the mean pulp-velocity of each stream.

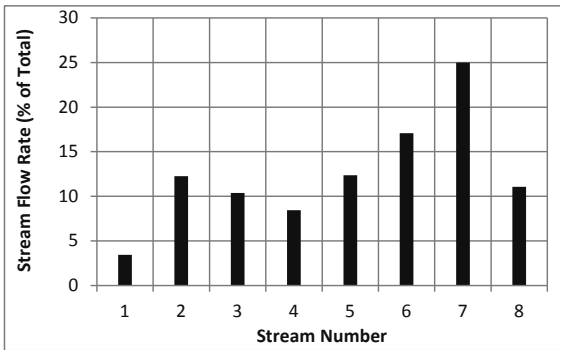

Fig. (9) *The predicted values of stream flow-rate, at 15 % solids.*

STABILITY OF SOLID DISTRIBUTIONS

Solid distributions stability means the distributions at the steady-state condition or the final distributions at the end of the spiral trough. It is very important to investigate and predict the number of turns that is required for the stability of solid distributions. The number of enough spiral turns fulfills when the solid distributions become constant and do not change with increasing the number of turns. The constant solid distribution fulfills when agreement between predicted values of any spiral turn and stability distribution of spiral outlet is satisfied. In this study, the stability distribution is taken as the solid distribution at the end of the sixth turn of the spiral separator. This is because LD9 spiral separator has only six turns.

The stability of solid distribution is predicted using two cases of solid percent, namely: 0.3% and 15%at flow rate of 6 m^3/hr. For the above purpose, solid distributions on the spiral trough were chosen at the outlet of each spiral turn. The solid distributions of cases 0.3% and 15% solids are shown in Figs. (10) and (11), respectively.

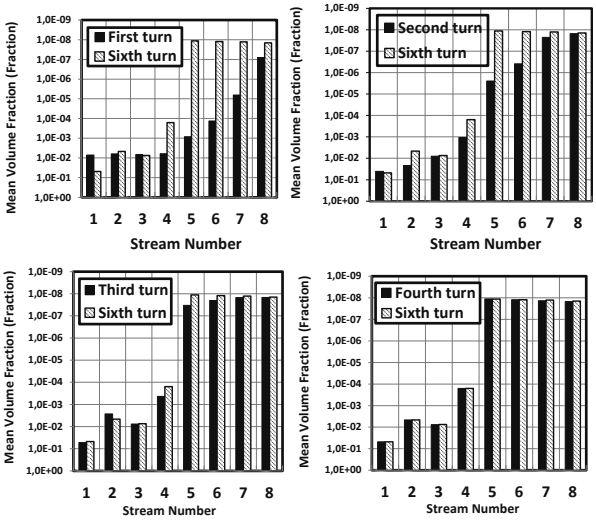

Fig. (10) *Change of the solid distributions with the number of turns at 0.3% solids and 6 m^3/hr flow rate.*

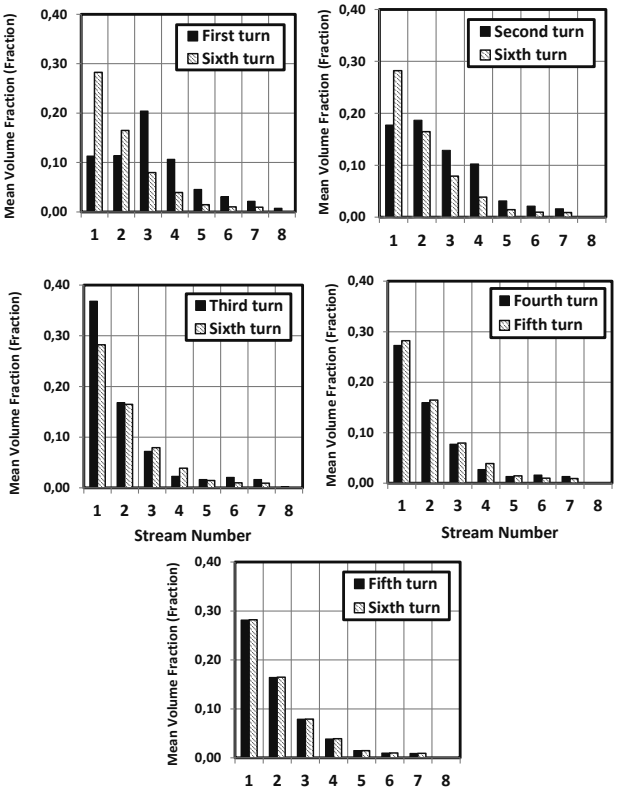

Fig. (11) *Change of the solid distributions with the number of turns at 15% solids and 6 m³/hr flow rate.*

Figures (10) and (11) show the solid distributions as a volume fraction. After the first spiral turn, the solid distributions are greater than the final distribution in the outer region of the spiral trough, while, it is lower in the inner region. It means that the particulate-flow moves toward the outer part of trough at the end of the first turn. After the second spiral turn, the deviation between solid distribution and final (stability) distribution decreases comparing to the first turn. After the third spiral turn, the agreement between water depth and stability depth is about 95% in case of 0.3% and less than 95% in case of 15% solids. After the fourth turn, a complete agreement between the solid distributions and stability distributions is achieved in case of 0.3% solids while the complete agreement in case of 15 % solids is satisfied after the fifth turn. This means that four turns of LD9 spiral separator are enough for the stability of the solid distributions in case of 0.3 % solids and five turns is required for stability in case of 15% solids. This point guides the designers to the suitable number of turns that is enough for the stability of solid distributions. This concept is very important for designers and operators.

CONCLUSIONS

From this study, the following conclusions can be stated:

1. The suggested numerical model can be applied for any spiral separator after modifying the domain geometry to the required separator.
2. To improve the agreement between the predicted and the experimental results, the experimental free-surface profile was used to complete the computational domain. This achieved a good agreement between the model predictions and the experimental results. Thus, validation of the particulate-flow model is satisfied.
3. The number of turns required to reach the steady-state of particle size distribution increases with increasing the solid content of the feed pulp.

REFERENCES

1. Burch CR (1962). Helicoid Performance and Fine Cassiterite-Contributed Remarks. Trans. Inst. Min. Metall.71:406-415.
2. Doheim MA, Abdel Gawad AF, Mahran GMA, Abu-Ali MH , Rizk AM(2013). Numerical Simulation of Particulate-Flow in Spiral Separators: Part I, low solids Concentration (0.3 & 3% solids). Applied Mathematical modeling 37(1):198-215.
3. Escue A, Cui J(2010). Comparison of turbulence models in simulating swirling pipe flows. Applied Mathematical Modelling 34(10) :2840–2849.
4. Ferziger,J. H. and Peric, M.,(1999). Computational methods for fluid dynamics. Second edition, Springer.
5. Fluent 6.3.26 User's Guide (2006), www.fluentusers.com, Fluent Inc., USA.
6. Holland-Batt AB, Holtham PN (1991). Particle and Fluid Motion on Spiral Separators. J.Minerals Engineering 4(3-4): 457-482.
7. Holland-Batt, A. B. (1995) .Some design considerations for spiral separators. Minerals Engineering, Vol. 8, No. 11 pp.1381-1395.
8. Holtham PN (1992). Particle transport in gravity concentrators and the Bagnold effect.Minerals Engineering 5(2): 205-221.
9. Holtham PN (1997). Experimental validation of a fundamental model of coalspirals. Australian Coal Association research program (ACARP).
10. Jancar T, Fletcher CAJ, Holtham PN, Reizes JA (1995). Computational and Experimental Investigation of Spiral Separator Hydrodynamics. Proc. XIX Int. Mineral Processing Congress, San Francisco, USA.
11. Jancar ML, Holtham PN, Davis JJ, Fletcher CAJ. (1995). Approaches to the development of coal spiral models. An International symposium, Soc. Mining, Metal and Exploration, Littliton, USA, pp. 335-345.
12. Kuang S, , Qia Z, Yua AB, Vinceb A, Barnettc GD, Barnettc PJ(2014). CFD modeling and analysis of the multiphase flow and performance of dense medium cyclones. Minerals Engineering 62:43–54.
13. Loveday GK, Cilliers JJ (1994). Fluid flow modelling on spiral concentrators. Minerals Engineering, Vol. 7, Nos. 2-3, pp. 223-237.
14. Machunter DM., RichardsRG, Palmer M K (2003). Improved gravity separation systems utilizing spiral separators incorporating new design parameters and features", Heavy Minerals Conference (HMC) 2003,Johannesburg, South African Institute of Mining and Metallurgy,2003
15. Matthews BW, Fletcher CAJ, Partridge AC (1998b). Computational Simulation of Fluid and Dilute Particulate Flows on Spiral Concentrators. Applied Mathematical Modelling 22 :965-979.
16. Matthews BW, Fletcher CAJ, Partridge AC, Vasquez S (1999a). Computations of Curved Free Surface Water

Flow on Spiral Concentrators. J. Hydraulic Engineering 125 (11):1126-1139.
17. Mathews BW, Fletcher CAJ, Partridge TC (1999b). Particle Flow Modeling on spiral concentrators: Benefits of dense media for coal processing?. Second International Conference on CFD in the Minerals and Process Industries, CSIRO, Melbourne, Australia, 6-8 December, 1999.
18. Matthews BW, Holtham P, Fletcher CAJ, Golab K, Partridge AC,(1998a). Computational and Experimental Investigation of Spiral Concentrator Flows. Coal 1998: Coal Operators' Conference, University of Wollongong & the Australasian Institute of Mining and Metallurgy, 415-421.
19. Mishra BK, Tripathy A (2010). A preliminary study of particle separation in spiral concentrators using DEM. International Journal of Mineral Processing 94(3-4):192–195.
20. Radman JR, Langlois R, Leadbeater T , Finch J, Rowson N, Kristian Waters K (2014). Particle flow visualization in quartz slurry inside a hydrocyclone using the positron emission particle tracking technique. Minerals Engineering 62: 142–145
21. Stokes YM, Wilson SK, Duffy BR (2004). Thin-Film Flow in Open Helically-Wound Channels. 15th Australasian Fluid Mechanics Conference, 13-17 December 2004,The University of Sydney, Sydney, Australia.
22. Wang JW, Andrews JRG (1994). Numerical Simulations of Liquid Flow on Spiral Concentrators. J. Minerals Engineering 7(11):1363-1385.
23. Yakhot V, Orszag SA (1986). Renormalization Group Analysis of Turbulence I. Basic Theory. Journal of Scientific Computing 1 (1): 1-51.